Stoch Environ Res Risk Assess (2009) 23:275–288
DOI 10.1007/s00477-008-0214-x

ORIGINAL PAPER

Analysis of forest thinning strategies through the development of space–time growth–interaction simulation models

Eric Renshaw · Carlos Comas · Jorge Mateu

Published online: 26 January 2008

Abstract Thinning strategies are a prime factor in generating spatial patterns in managed forests, and have a dramatic effect on stand development, and hence product yields. As trees generally have long life spans relative to the length of typical research projects, the design and analysis of complex long-term spatial–temporal experiments in forest stands is clearly difficult. This means that forest modelling is a key tool in the formulation and development of optimal management strategies. We show that the highly flexible Renshaw and Särkkä algorithm for modelling the space–time development of marked point processes is easily adapted to enable the comparative study of different thinning regimes. This procedure not only provides a powerful descriptor of forest stand growth, but there is considerable evidence that it is particularly robust to the accuracy of model choice. Two distinct thinning approaches are considered in conjunction with a variety of tree growth functions and both hard- and soft-core interaction functions. The results obtained strongly suggest that combining the immigration–growth–spatial interaction model with spatially explicit thinning algorithms produces a realistic and flexible mechanism for mimicking real forest scenarios.

E. Renshaw (✉)
Department of Statistics and Modelling Science,
University of Strathclyde, Livingstone Tower,
26 Richmond Street, Glasgow G1 IXH, UK
e-mail: eric@stams.strath.ac.uk

C. Comas · J. Mateu
Department of Mathematics, Universitat Jaume I,
Campus Riu Sec, E-12071 Castellón, Spain
e-mail: comas@sg.uji.es

J. Mateu
e-mail: mateu@mat.uji.es

Keywords Forest modelling · Marked point processes · Spatially explicit forest dynamics · Thinning strategies · Distance-dependent forest models

1 Introduction

Several previous forest studies have suggested that thinning strategies are a prime factor in generating spatial forest patterns (see Penttinen et al. 1992; Särkkä and Tomppo 1998; Tomppo 1986). However, although this forest operation has a dramatic impact on both future stand development and product yields, in relative terms little attention has been paid to the modelling of such managed operations (see, for instance, Pukkala and Miina 1998; Pukkala et al. 1998; Courbaud et al. 2001; Raulier et al. 2003). The difficulty of obtaining experimental data to study the effects of distinct thinning strategies, primarily due to trees having a long life span, has clearly limited the analysis of this key element in silviculture.

Forest modelling allows us to examine various thinning strategies and to improve our understanding of the relationship between stand structure and stand dynamics under different forest scenarios. Over the past few decades, a large number of growth-yield models have been developed to describe forest dynamics based on individual tree information. Examples include: distance-independent models, such as the PROGNOSIS model (Stage 1973; Wykoff et al. 1982); its successors, namely the Forest Vegetation Simulator (Teck et al. 1996) and PROGNAUS (Monserud and Sterba 1996; Sterba and Monserud 1997); distance-dependent forest formulations, including FOREST (Ek and Monserud 1974), MOSES (Hasenauer 1994; Hasenauer et al. 1995), SILVA (Pretzsch 1992; Pretzsch et al. 2002) and SORTIE (Pacala et al. 1993), based on the JABOWA-

FORET family of models; and, the forest simulator proposed by Pukkala et al. (1998). However, although some of these models have been applied to predict resource availability in classical management contexts, they have rarely been used as tools to analyse how forest management can affect forest dynamics (Pukkala et al. 1998).

Typically, distance-dependent tree-level models (i.e. where trees are the basic unit of analysis) require tree coordinates as well as individual tree variables, such as height, trunk and crown diameter, in order to simulate forest growth. As such, a natural way to describe and analyse forest dynamics is through the development of spatial marked point processes, where points and marks can be easily associated with tree positions and features such as diameter and height. A realisation of a stochastic spatial marked point process consists of a set of points $\{x_i\}$ in a bounded region, which take the associated marks $m(x_i)$ (Stoyan et al. 1995). Although marked point process theory, as applied to forestry, has focused attention on the understanding of forest pattern in order to expose possible biological and forest-ecological generating mechanisms (e.g. Penttinen et al. 1992; Rathbun and Cressie 1994; Särkkä and Tomppo 1998; Mateu et al. 1998; Degenhardt 1999), rather less attention has been paid to the simulation of such patterns in order to gain a better understanding of forest space–time growth (Renshaw and Särkkä 2001; Comas and Mateu 2006).

Another important shortcoming in marked point process theory is that relatively few studies have weighted space and time equally; most prioritise on purely spatial structure, in contrast to real-life tree populations which evolve dynamically through time. To remedy this deficiency, Renshaw and Särkkä (2001), henceforth denoted (R&S), develop a continuous space–time stochastic process on the unit torus to generate spatial patterns of marked points evolving through time. This approach represents a reasonable approximation of a forest, where trees grow and interact continuously, and it can be easily adapted to encompass many realistic, practically oriented, scenarios (Comas 2005). Whilst other formulations include: the point processes of Hawkes (1971a, b; 1972), which were conceived to generate cluster configurations assuming an evolutionary structure in the point pattern; and, multi-generation point processes (Diggle 2003; Comas and Mateu 2006) which generate point patterns evolving through discrete time. Neither of these last two formulations have been applied to real forest scenarios.

The objective of this paper is to highlight how a wide variety of forest thinning strategies may be constructed, and subsequently compared, by generating marked point process patterns through the R&S spatio-temporal process. Our approach involves the incorporation of an explicit thinning, i.e. tree removal, algorithm in the growth–interaction stage, based on distance-dependent tree information. This enables us to have direct control over the thinning operation, thereby providing greater understanding of real forest dynamics under distinct thinning strategies.

2 The Spatial–temporal growth–interaction model

Combining distance-dependent forest models with spatially explicit thinning algorithms has already been shown to be a powerful tool to aid and improve forest management decision processes (Pukkala et al. 1998). In the R&S model a stochastic arrival-death process is combined with a deterministic growth–interaction process. The former provides an appropriate level of randomness and the latter a fast and efficient way of incorporating space–time interaction between (potentially) all the individuals present. Although their construct is totally general, they use simple illustrations to illustrate how the procedure may be applied in practice, and we adopt the same strategy here. For in any given forestry situation the examples used may be easily replaced by (if necessary) more complex processes relevant to the particular scenario under investigation.

First consider the stochastic mechanism that determines the arrival, location, initial mark size and death rates. This can clearly be as complex as deemed necessary. Indeed, we could have a general non-linear birth-immigration-death-mark size process coupled with a density dependent and anisotropic (i.e. direction dependent) location variable, either within the study region in the case of immigration, or centred around parent marks in the case of birth. However, since the simple immigration-death process has already been used successfully as a basic portrayer of stochastic population development, we shall retain it here. Further, we shall assume that immigrants are uniformly distributed over the study region, with initial mark size being either fixed or else uniformly distributed over a given range. So new immigrants k, arrive according to a Poisson process with rate α, are located within the study region, and either take variable marks $\tilde{m}_k = U(0, \epsilon)$ for some small $\varepsilon > 0$, or fixed marks $\tilde{m}_k = \epsilon$. Moreover, we presume that each individual tree may die "naturally" at rate μ; though it is trivial to generalise this to a density-dependent death rate.

In the R&S process, each mark changes size at times $t = dt, 2dt, \ldots$ through the *deterministic* incremental size change

$$m_i(t+dt) = m_i(t) + f(m_i(t))dt + \sum_{j \neq i} h(m_i(t), m_j(t); \|x_i - x_j\|)dt. \quad (2.1)$$

Here, $\|x_i - x_j\|$ denotes the distance between different individuals (i.e. points) i and $j \neq i$, $f(\cdot)$ denotes the mark growth function in the absence of spatial interaction, and

$h(\cdot)$ is an appropriate spatial interaction function taken over all points $j \neq i$. If $m_i(t + dt) \leq 0$ then the individual is deemed to have died "interactively" and the point i is deleted, as also happens for natural death.

2.1 Growth functions

The simplest forms of growth function, namely $f(m_i(t)) = \lambda$ and $f(m_i(t)) = \lambda m_i(t)$, corresponding to constant and multiplicative growth, respectively, clearly lead to marks growing without bound in the absence of spatial interaction. Since $f(\cdot)$ can exert a considerable influence on the generated pattern structure, care must be taken to choose stable forms, and two simple functions that remain bounded are

$$f_1(m_i(t)) = \lambda m_i(t)(1 - m_i(t)/K) \quad \text{and} \quad f_2(m_i(t)) = \lambda(1 - m_i(t)/K), \tag{2.2}$$

for intrinsic rate of growth λ and (non-spatial) carrying capacity K. These correspond to the classic logistic growth and immigration-death processes, respectively, and can be easily modified to suit specific situations.

These linear and quadratic forms are both special cases of the logistic power-law process

$$dm(t)/dt = am(t) - d[m(t)]^{p+1}, \tag{2.3}$$

which has the solution (e.g. Banks 1994)

$$m(t) = K[1 + ce^{-apt}]^{-1/p} \tag{2.4}$$

where the carrying capacity $K = (a/d)^{1/p}$ and $c = [K/m(0)]^p - 1$. For Eq. (2.3) reduces to the pure logistic form when $a = \lambda$, $d = \lambda/K$ and $p = 1$, and the linear form when $a = -\lambda/K$, $d = -\lambda$ and $p = -1$. As well as providing an extremely useful descriptor for modelling the dynamics of insect populations (Matis et al. 1998, 2007), in which the more aggressive the insect the higher the value of $p > 1$, the general representations (2.3) and (2.4) have also played a pivotal role in the modelling of tree growth. For they specifically equate to the Von Bertalanffy–Chapman–Richards growth function (VBCR)

$$f_3(m_i(t)) = a_0 m_i(t)^{a_1} - a_2 m_i(t) \tag{2.5}$$

(von Bertalanffy 1949; Richards 1959; Chapman 1961), which is used extensively to model both diameter (e.g. Prévosto et al. 2000) and height growth (e.g. Pienaar and Turnbull 1973). Here $a_0 = \beta K^v/v$, $a_1 = (1-v)$ and $a_2 = \beta/v$ (Lei and Zhang 2004), where K denotes the tree-size carrying capacity, β scales the time axis, and v is a parameter that defines the curve shape (i.e. an allometric constant). Note the implicit sign change between (2.3) and (2.5); in the former the power term $dm(t)^{p+1}$ "controls" the linear growth term am, whilst the converse holds in the latter. Moreover, for $a_0, a_2 > 0$ (i.e. $\beta/v > 0$) and small $m(0) \simeq 0$, the rate of growth

$$dm(t)/dt = a_0 m(t)^{1-v} - a_2 m(t) \simeq \begin{cases} am(t)^{1-v} \simeq 0 & \text{if } 0 < v < 1 \\ a/m(t)^{v-1} \sim \infty & \text{if } v > 1, \end{cases} \tag{2.6}$$

so only the case $0 < v < 1$ makes "practical sense" when $m(0)$ is small. Clearly, the $v > 1$ case should only be used in situations which do not involve very small trees. Moreover, as the second derivative $d^2m(t)/dt^2 = 0$ at $\ln(m(t)) = (a_2/a_0)/[v(v-1)]$, it follows that the condition for having a point of inflexion at $m(t) = \tilde{m}$ for some $0 < \tilde{m} < K$ is that

$$-\infty < (a_2/a_0)/[v(v-1)] < \ln(K). \tag{2.7}$$

In such situations Eq. (2.3) produces a sigmoid curve with an upper asymptotic value K, i.e. the classical scenario extensively applied in biology and in forest growth modelling (Pienaar and Turnbull 1973).

2.2 Spatial interaction functions

Not only is the choice of possible growth functions large, but the number of potential spatial interaction functions is also big. So their combination gives rise to a huge range of models. All we shall do here is to highlight two or three, and to repeat that the resulting simulation algorithm is totally flexible in its applicability. Following R&S, first consider the symmetric hard-core interaction function

$$h_1(m_i(t), m_j(t); \|x_i - x_j\|) = -bI(\|x_i - x_j\| < r(m_i(t) + m_j(t)), \tag{2.8}$$

where the indicator function $I(F) = 1$ if F is true and $I(F) = 0$ otherwise. We assume that the area, in horizontal projection, over which the mark $m_i(t)$ competes for resources, i.e. its influence zone, can be represented by a disk of radius $rm_i(t)$. Thus r is the scaling parameter that relates say tree height or diameter to canopy radius. As soon as two disks overlap, i.e. $\|x_i - x_j\| < r(m_i(t) + m_j(t))$, then competitive interaction takes place with force b. Since this function is symmetric, the larger and smaller of an interactive-pair are affected equally, and although this form represents a reasonable approximation for interaction between marks of similar size it may be inappropriate if $m_i(t)$ and $m_j(t)$ are radically different. For then the smaller mark can exert an appreciable influence on the growth of the larger mark irrespective of how tiny it may be.

To construct a soft-core form that takes account of the relative sizes of two interacting marks, suppose that the amount of competition experienced by a given mark is a

function of the extent to which its influence zone overlaps those of neighbouring marks (Staebler 1951). Then we may take the interaction function to be proportional to the relative size of the influence zone (Gerrard 1969). Let $D(x_i,s)$ denote the disk with centre x_i and radius s, and place

$$h_2(m_i(t),m_j(t);\|x_i-x_j\|) = -b\ \text{area}\{D(x_i,rm_i(t)) \cap D(x_j,rm_j(t))\}/(\pi r^2 m_i^2(t)). \tag{2.9}$$

Thus now the smaller of two interacting marks is affected substantially more than the larger, whilst marks of equal size are affected equally. So this function clearly has particular application to many real-life growth–interaction scenarios. In particular, it promotes asymmetric effects, since larger trees have a competitive advantage over smaller ones; trees with similar size experience similar spatial inhibition. This Gerrard-based function and its modifications (see also, Bella 1971) have been used as measures of tree competition in the FOREST model (Ek and Monserud 1974) and in its successors MOSES (Hasenauer 1994; Hasenauer et al. 1995) and SILVA (Pretzsch 1992; Pretzsch et al. 2002).

Extensions are clearly endless. For example, an extreme version of one-sided interaction, i.e. a large mark influences a small mark but not vice versa, is easily constructed by replacing $h_1(\cdot)$ by

$$h_3(m_i(t),m_j(t);\|x_i-x_j\|) = -bI\{\|x_i-x_j\|<r(m_i(t)+m_j(t))I(m_j(t)>m_i(t))\}. \tag{2.10}$$

So locally dominant marks will not now decline as smaller fresh immigrants pack in around them.

2.3 Interplay between growth and interaction

To appreciate the interplay between the growth and interaction functions, suppose that mark i lies within the zone of influence of θ neighbouring discs under the hard-core regime $h_1(\cdot)$. Then on letting $dt \to 0$, the growth–interaction equation (2.1) reduces to

$$dm_i(t)/dt = \begin{cases} \lambda m_i(t)(1-m_i(t)/K) - b\theta & (\text{under } f_1) \\ \lambda(1-m_i(t)/K) - b\theta & (\text{under } f_2). \end{cases} \tag{2.11}$$

Taking f_1 first, we see that for $m_i(t)$ to survive we require

$$dm_i(t)/dt = \lambda m_i(t)(1-m_i(t)/K) - b\theta > 0. \tag{2.12}$$

Hence as $dm_i(t)/dt = 0$ at $m_i(t) = (m',m'') = (K/2)[1 \pm \sqrt{1-4b\theta/(\lambda K)}]$, it follows that if $m_i(t) < m'$ then $m_i(t)$ decays to zero, if $m' < m_i(t) < m''$ then $m_i(t)$ grows to m'', whilst if $m_i(t) > m''$ then $m_i(t)$ decreases to m''. This presupposes, of course, that $\sqrt{1-4b\theta/(\lambda K)}$ is real, i.e. that $\theta \le \lambda K/4b$. So for $m_i(t)$ to be able to survive within even a single zone of influence (i.e. $\theta = 1$) we need the number of interaction discs, b, to be less than $\lambda K/4$. In contrast, under f_2 we see that $dm_i(t)/dt \uparrow \lambda - b\theta$ as $m_i(t) \to 0$. So now tree i's survival depends purely on whether the number of covering discs, θ, is less than λ/b, and not on the size of $m_i(t)$.

In reality, if a small $m_k(t)$ is affected by a larger $m_i(t)$, then that, in turn, will be affected by $m_k(t)$ and so reduce in size. So suppose that under the model (f_2,h_1) we have $\lambda < b$, so that no mark can survive under a covering disk. Then if marks $m_i(t) > m_k(t)$ interact at time $t = 0$, but $rm_i(t) < \|i-k\| < r(m_i(t)+m_k(t))$, both $m_i(t)$ and $m_k(t)$ will decrease until their two discs just touch, at which point $m_k(t)$ will start to increase, and $m_i(t)$ decrease, until $m_i(t) = m_k(t)$. If, however, $rm_i(t) > \|i-k\|$, then k's survival depends on whether it is uncovered by $m_i(t)$'s shrinking zone of influence before it dies. A little algebra shows that k dies under the influence of i if the inter-point distance

$$\|i-k\| < r\phi[m_i(0)-m_k(0)]/[m_k(0)+\phi] \quad \text{where } \phi = (K/\lambda)(b-\lambda). \tag{2.13}$$

A similar examination of the VBCR growth function, which has probably been employed more than any other in studies of trees and stand growth (Zeide 1993), shows that a small tree i will survive if and only if

$$dm_i(t)/dt = a_0 m_i(t)^{a_1} - a_2 m_i(t) - b\theta > 0. \tag{2.14}$$

Whence we see that for small marks $m(t) \simeq 0$:

(i) if $0 < v < 1$ then $dm(t)/dt \simeq am(t)^{1-v} - b\theta < 0$,
(ii) if $v = 1$ then $dm(t)/dt \simeq a - b\theta < 0$ if $b > a/\theta$,
(iii) if $v > 1$ then $dm(t)/dt \simeq a/m(t) \gg 1$.

To illustrate these three scenarios suppose we take $\lambda = \beta = 1$ and $K = 25$, with:

(i) $v = 1/2$: then $a_0 = \beta K^v/v = 10$, $a_1 = 1-v = 1/2$ and $a_2 = \beta/v = 2$. So as $dm(t)/dt = 10\sqrt{m(t)} - 2m(t) - b\theta = 0$ at $m(t) = (m',m'') = [2.5\{1 \pm \sqrt{1-0.08b\theta}\}]^2$, it follows that if $m(t) < m''$ then $m(t)$ decays to zero, if $m'' < m(t) < m'$ then $m(t)$ grows to m', whilst if $m(t) > m'$ then $m(t)$ decreases to m'. Thus under high intensity packing it is not really possible to have a lower canopy structure containing very small established small trees. In contrast, consider

(ii) $v = 1$: so $dm(t)/dt = 25 - 2m(t) - b\theta$, whence $dm(t)/dt > 0$ provided $b\theta < 25$. Thus whereas any small tree having mark $m(t) < m''$ dies under (i), under (ii) a lower canopy structure can clearly become established. Finally, suppose

(iii) $v = 2$: now $dm(t)/dt = K^2/(2m(t)) - (m(t)/2) - b\theta = 0$ at $m(t) = (m''', m^{iv}) = \pm\sqrt{K^2 + b^2\theta^2} - b\theta$, and as $m''' < 0$ this means that any $m(t) > 0$ under interaction pressure $b\theta$ converges to $m^{iv} > 0$. So under this regime it is not possible for a lower canopy to become established. Clearly, the parameter v plays a crucial role in the determining the type of canopy structure generated by the model.

3 Adapting the model to real forest scenarios

For any given choice of growth and interaction functions, $f(\cdot)$ and $h(\cdot)$, and data comprising tree locations and their corresponding mark values, we can always estimate the parameters employed in the model (2.1). R&S use a maximum pseudo-likelihood approach for patterns that are sampled at *fixed* time points; whilst Särkkä and Renshaw (2006) [S&R] develop a least squares estimation procedure for estimating parameters of the process based on *successive* time points. The reasons which underlie this change of approach are twofold. First, when estimating parameters *through time*, likelihood based approaches would incur far higher computational demands than their least squares counterparts. Second, use of simple stochastic examples (in S&R) demonstrates that least squares methods can be as powerful as likelihood-based approaches, as well as being mathematically simpler. Nevertheless, having obtained parameter estimates we are still faced with the problems of (a) selecting the "best" growth and interaction functions to apply in a given forest situation, and (b) "testing" to see whether the constructed model represents a realistic and useful approximation to reality. To date, both questions have been answered on a purely subjective assessment based on comparing real and simulated data plots "by eye". The development of a robust statistical procedure for tackling such issues remains an open, and extremely important, question for future investigation.

It is vitally important to ensure that as much knowledge of forest development as possible is enshrined in our chosen model structure. First, we need to relate our (theoretical) mark variables $m_i(t)$ to key features of tree development. Given that tree dbh (i.e. diameter at breast height) is highly affected by tree density, and so is very sensitive to forest management, it seems eminently reasonable to let $m_i(t)$ be directly proportional to this forest variable. So from now on, we denote $m_i(t) = \text{dbh}/2$ to be tree radius at breast height (rbh). Whence the stand basal area (sba) at time t is given by $G(t) = \pi \sum_{i=1}^{n} m_i^2(t)$, where n denotes the number of trees. Moreover, $G(t)$ can be easily related to an important element of stand growth, namely the quadratic mean diameter (qmd) $D(t) = 2\sqrt{G(t)/(\pi n)}$; usually quoted per-hectare as $D(t) = \sqrt{40,000G(t)/(\pi n)}$. The qmd is essential for estimating product yields, since it can be easily transformed into total biomass production, i.e. stand basal area, and also provides information about "average" tree size. Ek and Monserud (1974) consider tree influence zones to be proportional to the crown of a solitary tree, and so measure, in horizontal projection, tree competition for resources. Following this approach, we therefore take the theoretical disk of influence to be proportional to the horizontal projection of tree crown. That is, the crown radius for tree i at time t can be estimated via $\text{crown}_i(t) = \delta m_i(t)$, where δ is a constant of proportionality between rbh and crown radius.

Since the spectrum of a linear space–time growth–interaction model can be readily derived (Renshaw and Ford 1983; Renshaw 1984), comparison of empirical and theoretical spectra at the start of a forest investigation is an extremely useful way of obtaining initial estimates on the likely force and extent of between-tree interaction. However, more detailed spatial studies of forest configurations need to be undertaken if we are to derive estimates of, for example, maximum dbh, intrinsic rate of tree growth and spatial interaction effects. Though given that real forest mapped data are not common, we need to derive approximate values for these parameters both from the forest literature and from theoretical assumptions derived from the growth–interaction functions. It must be stressed that the aim of such a literature investigation is to obtain sensible forest values in order to obtain qualitatively "realistic" forest dynamics, rather than trying to determine accurate quantitative results, since these will clearly suit our simulation studies. Moreover, since conifer species have been extensively studied, given their economic importance and their abundance in the Northern Hemisphere, there already exists a vast database for them which facilitates our search for real forest parameters. We shall therefore base our parameter values on conifer species.

3.1 Tree carrying capacity K

The maximum attainable tree "size" K, is determined by the genetic nature of each individual and the overall forest area productivity, and is therefore highly local. However, for our simulation exercise, we shall select a sensible constant K-value from the forest literature in order to obtain qualitatively "realistic" forest dynamics. For instance, Pukkala et al. (1994) present 51 Scots pine plots and 48 Norway spruce plots of variable stand density and age, involving 1,622 pines and 2,478 spruces in total, for a case study in North Karelia in Finland. For these data the maximum recorded dbh for pine and spruce is around 50 cm (i.e. $K = 25$ cm), whilst the *maximum tree age*

based on the data is around 141 and 102 years, for pine and spruce, respectively. Although it is possible to find larger trees (say dbh $\simeq$75 cm) in very productive forest areas, these values do not represent the "typical" maximum tree dbh for "normal" European forest regions.

3.2 Allometric constant v

The allometric constant v is a shape parameter of the growth curve, and is essential for defining realistic growth patterns for forest and biological modelling. We have seen that to have a sigmoid curve with an upper asymptotic value K, a situation widespread in biology and forest growth modelling, expression (2.6) has to be satisfied with $a_0, a_2 > 0$. Moreover, expression (2.5) shows that only the case $0 < v < 1$ makes practical sense when $m(0)$ is small and $a_0, a_2 > 0$. Whence on rewriting (2.6) as

$$-\infty < K^{-v}/[v(v-1)] < \ln(K), \tag{3.1}$$

it follows that for any $K > 1$ there exists some $0 < v < 1$ such that expression (3.1) is always satisfied. So for $a_0,\ a_2 > 0,\ K > 1$ and $0 < v < 1$, the VBCR growth function (2.5) always possesses a point of inflection at some point $0 < \tilde{m} < K$. However, as seen in Sect. 2, the case $0 < v < 1$ does not favour the development of a genuine two-tier canopy structure, which is often found in real forest situations. Indeed, to generate this feature we require $v = 1$, when, in the absence of spatial interaction, individual tree growth rate decreases monotonically until the carrying capacity K is reached. In practice, however, such growth structure may not represent a realistic forest situation, since younger trees might be expected to grow faster than older ones. So in order to compare both growth patterns we shall consider two distinct v-regimes, namely $v = 1$ (linear approach to K) and $v = 0.7$ (sigmoid growth with a point of inflexion at $0 < \tilde{m} < K$).

3.3 Growth parameter β

Tree ring growth is usually maximised in the third year of seedling development. Growth then decreases, at first quite quickly, and then more steadily, once trees become older (Fritts 1976). This initial pattern can be easily approximated by exponential growth. Although this may be expected for young non-interacting trees, as soon as trees start to interact with each other then spatial interaction causes tree growth to decrease. One way of obtaining an "appropriate" value for β would be to perform a direct analysis on the VBCR growth function. However, even with the basic logistic process the estimation of parameters with small estimated standard errors, using say a likelihood or least squares approach, requires information on both the initial (transient) and later (persistent) periods of forest growth. Since the former is likely to be relatively weak, the estimate for β will be partially confounded with those for K and v, so all we can reasonably achieve is a rough value. Let us therefore choose β in order to best reflect the tree size attainable for a given tree age. In the database presented by Pukkala et al. (1994) the maximum recorded dbh is around 50 cm, with the maximum tree age lying in the range 102–141 years. Whence on presuming that trees with maximum dbh are also the older ones, we can select that value of β which enables trees to approach their maximum size (e.g. $m(t) = 0.95K$ or $0.99K$) at say $t = 120$ years.

The (non-spatial) VBCR equation (2.6) reduces to the logistic power-law process (2.3) when $a = -a_2$, $d = -a_0$ and $p = a_1 - 1$. Whence on substituting for $a_0 = \beta K^v/v$, $a_1 = 1 - v$ and $a_2 = \beta/v$ (Lei and Zhang 2004) into the general solution (2.4), it follows that the resulting growth equation

$$dm(t)/dt = -(\beta/v)m(t) + (\beta K^v/v)m(t)^{1-v} \tag{3.2}$$

takes the solution

$$m(t) = K[1 + \{(m(0)/K)^v - 1\}\exp(-\beta t)]^{1/v}. \tag{3.3}$$

So on making the realistic assumption that $m(0) \simeq 0$, we see that for $m(t) = \gamma K < K$

$$\beta = -(1/t)\ln(1 - \gamma^v) \quad (v > 0). \tag{3.4}$$

Thus for $\gamma = 0.95$ and 0.99, i.e. a tree respectively attains 95 and 99% of its maximum rbh K after say $t = 120$ years, we have

v:	0.1	0.3	0.5	0.7	1	2
$\beta\,(\gamma = 95\%)$:	0.044	0.035	0.031	0.028	0.025	0.019
$\beta\,(\gamma = 99\%)$:	0.058	0.048	0.044	0.041	0.038	0.033

(3.5)

For example, in the case of linear growth, comparing equations (2.2) and (2.5) shows that $v = 1$ and $\beta = \lambda/K$. So we need $\lambda = 0.63$ or 0.95 for $m(t)$ to reach 95% or 99%, respectively, of its maximum attainable rbh of $K = 25$ cm after 120 years.

3.4 Interaction parameter b

If tree crowns tend to overlap with each other, then spatial inhibition forces can be presumed to be "weak"; i.e. b is "small". Conversely, spatial interaction can be presumed to be "strong", and larger values of b may be assumed. Although detailed study of real forest configurations should be undertaken to obtain good estimates of b, a lack of mapped data means invoking a more pragmatic approach. Spatial interaction dynamics are highly

related to tree tolerance to shade, an important concept in silviculture. Species that can survive under more shaded conditions than others, since their leaves are able to photosynthesise more efficiently at lower light intensities, are described as shade-tolerant species (Oliver and Larson 1996). Either full shade or full sunlight conditions create very demanding forest microclimates where only adapted species can withstand these extreme conditions. For instance, shade-intolerant species (e.g. pines) cannot survive in low sunlight since they are unable to balance their positive photosynthesis/respiration rate; this characteristic is fully dependent on the tree development stage (Wahlenberg 1960). Certain pine species, such as the loblolly (*Pinus taeda* L.) and shortleaf (*P. echinata* Mill.) pines can initially survive under a dense canopy, though after several years seedlings need to be released from any overstory (i.e. forest upper canopy) if the stand is to survive (Ferguson 1963). As such, the tolerance of seedlings to shade can be used to obtain an approximate value of the interaction effect b.

To illustrate this approach consider the seedling tolerance to shade of an extensively studied conifer species, namely Scots pine (*Pinus Sylvestris L.*), which can withstand certain levels of shadow, though it grows best in bright sunlight. Now we see from Eq. (2.14) that a small tree or seedling of size m will survive under θ zones of influence if and only if

$$dm_i(t)/dt = a_0 m_i(t)^{a_1} - a_2 m_i(t) - b\theta > 0. \tag{3.6}$$

Whence on taking $a_0 = \beta K^{\nu}/\nu$, $a_1 = 1-\nu$ and $a_2 = \beta/\nu$, it follows that survival, i.e. $dm_i(t)/dt > 0$, requires

$$b < (\beta m/(\theta\nu))[(K/m)^{\nu} - 1]. \tag{3.7}$$

Whilst θ denotes the number of interacting neighbours under the symmetric hard-core interaction function h_1 (see (2.8)), for the asymmetric area-interaction function h_2 (see (2.9)) θ relates to the fraction of crown covered by other crowns. For given K and γ there are clearly a wide range of possible (β,ν)-values that enable condition (3.7) to be satisfied. Suppose we retain $K = 25$ cm together with the scenarios $\gamma = 0.95$ and 0.99 and $\nu = 0.7$ and 1. Then on recalling (3.5), we see from (3.7) that survival under a single zone of influence (i.e. $\theta = 1$) requires that for:

ν	γ	β	b
0.7	0.95	0.028	<0.339
0.7	0.99	0.041	<0.503
1.0	0.95	0.025	<0.599
1.0	0.99	0.038	<0.921

So a suitably wide set of b-values that relate to fairly strong interaction effects would be 0.3, 0.45, 0.55 and 0.9, respectively.

4 Thinning strategies

The yield of commercial timber volume within a given stand can be substantially increased by applying intermediate forest cuttings in order to control stand density. For reducing tree–tree competition promotes a positive tree growth response by increasing free space: this concentrates timber production in selected trees, which in turn increases the overall financial return. In some cases this artificial tree selection mimics the natural elimination of trees suppressed by an early and accelerated tree removal, yielding forest outputs such as pulp wood and fuel wood. Smith et al. (1997) define a "thinning programme" as a series of tree density reductions, through time, which maximises the timber production in the whole forest rotation (i.e. the total time a single forest is allowed to grow). It comprises the tree selection (or removal) criterium, the thinning regime (i.e. the number of cuttings per forest rotation), and the thinning weight or severity (i.e. the number of stems to be removed in each thinning).

4.1 Methods of thinning

Four main thinning procedures are used in the tree selection process, namely: (1) thinning from below; (2) thinning from above; (3) selection thinning; and, (4) systematic thinning. Combining these methods yields a wide variety of intermediate methods that are usually called "mixed thinnings". Thinning from below (a.k.a German or low thinning) favours the upper crown classes (comprising dominant and co-dominant trees) by removing trees from the lower crown classes which comprise intermediate, i.e. suppressed, trees and overtopped, i.e. completely suppressed trees. So it tries to mimic natural selection by favouring vigorous trees and accelerating the mortality of suppressed ones. In contrast, thinning from above (a.k.a. French, crown or high thinning) tends to favour the growth of "promising" target trees from the upper crown class by removing trees from the same crown class. It therefore regulates tree competition by eliminating strong competitors rather than by removing weak ones, as is the case when thinning from below. This selection criterium has a strong control on tree competition, for irrespective of the thinning severity, tree removal is restricted to the upper crown class and so no trees are removed from lower hierarchic positions. After a crown thinning the forest usually becomes separated into two canopies: a favoured upper canopy consisting of dominant and co-dominant trees; and, a lower canopy comprising intermediate and overtopped trees. Selection thinning favours the lower crown classes by removing trees from the upper crown classes; poorly formed dominant trees are removed in order to stimulate

the growth of potential target trees in the lower classes. Finally, systematic thinning involves pre-determining the tree–tree spacing configuration, i.e. the spatial *point* structure, rather than the tree hierarchic, i.e. *mark*, position in the canopy. This type of thinning is easy to apply, and can be advantageous over other types of thinning when applied to young forests where hierarchic position is not yet established.

4.2 Thinning severity

A popular method to determine the thinning severity, defined by the percentage of trees removed from each crown class, involves considering the change in *relative spacing*, initially formulated by Hart (1928). The Hart–Becking spacing index is defined by the average distance between trees, expressed as a proportion of dominant stand height. Conditional on regular tree spacing, this index takes the form

$$S = \left(\sqrt{10,000/n}\right)/H, \tag{4.1}$$

where S is the relative spacing index, and n and H denote the number of trees per-hectare and the dominant stand height, respectively. If S is specified a priori, then expression (4.1) yields the residual tree density remaining after thinning. Whilst for given n, it provides a simple inverse relationship between S and H which indicates when the forest should be thinned. Note that the stand basal area (per-hectare) has also been extensively used to specify thinning weight, and defines the thinning severity in terms of the sum of individual tree trunk sections measured at breast height. So as it easily relates both to stand volume and individual tree size, it enables us to define the thinning severity in terms of both stand volume and the number of trees. However, care must be taken when thinning, as it does not always lead to an increase in commercial timber volume. For in some cases, a reduction in tree density can produce negative effects due to thinning stress, rather than favouring the growth of the remaining trees. This happens, for example, when they are in poor physiological condition, and the forest stand is affected by strong winds and frequent frosts.

5 Illustrating spatial–temporal dynamics of forest thinning

We have already shown in Sects. 2 and 3 that the general growth–interaction model (2.1) is highly flexible. Indeed, by changing the growth and interaction functions, $f(\cdot)$ and $h(\cdot)$, we can generate a wide variety of different pattern structures (see R&S and S&R for examples). Moreover, a considerable number of thinning strategies may be applied in each case. So the potential number of growth–interaction-thinning regimes is clearly immense. Thus all we can do here is to illustrate the simulation approach through a small number of examples, and stress that the approach is totally general both in its usefulness and its applicability.

5.1 Simulation algorithm

Extending the approach taken by R&S and S&R yields the following simulation algorithm. Population updates to each of the n marks are made at the discrete set of times dt,$2dt$,..., where $dt \ll 1$ (usually $dt = 0.01$ or 0.001) and U denotes a sequence of independent $U(0,1)$ random variables. For demonstration purposes we assume that immigration occurs randomly at rate α, though this could easily be replaced by say a replacement planting strategy if required, and that natural death occurs at rate μ. Encompass the stand area by a rectangle of size $r \times s$. Then for a sequence of uniform $U(0,1)$ random numbers, $\{U_j\}$, consider the following procedure:

cycle over time $t = dt,2dt,...$
- cycle over individuals $i = 1,...,n$
  - test for natural death: if $U_j \leq \mu dt$ then set $m_i = 0$
  - apply the growth–interaction function: use expression (2.1) to determine $m_i(t + dt)$ from $m_i(t)$
  - test for *potential* new immigrants: if $U_{j+1} \leq \alpha dt$ then add new mark $m_{n+1} = U(0,1)$ with carrying capacity K and location $x_{n+1} = (rU_{j+2}, sU_{j+3})$
  - accept or reject new immigrant: if x_{n+1} lies within the forest stand then *accept* and set n to $n + 1$; else *reject* x_{n+1}
  - reset spatial positions: if $m_i \leq 0$ then delete $(x_i; m_i)$ from list and relabel remaining marks with $j > i$ to $j-1$, and set $n \rightarrow n - 1$
- apply the selected thinning strategy if either: t corresponds to a "thinning-time"; or the spatial structure satisfies the 'thinning criteria'

if t is (say) integer then output $\{(i, x_i(t), m_i(t)): i = 1,...,n\}$.

Note this algorithm is easily altered to accommodate *any* variant of the growth, interaction, immigration, thinning, and indeed planting, regimes.

In order to demonstrate this approach we clearly need to choose an appropriate, spatially explicit, thinning algorithm based on the competitive status between trees. We shall adapt one developed by Pukkala et al. (1998) for a distance-dependent yield model for a mixed stand of Scots pine and Norway spruce, and consider explicit thinning procedures for optimising forest financial returns. In this

model the thinning programme is specified by the stand basal area that triggers the thinning, the tree removal percentage in different diameter classes, and an algorithm that computes the order in which trees are removed. Trees are successively removed based on a function of their diameter classes and the degree of spatial inhibition experienced (trees affected by strong interaction effects are selected first). Other computational methods to optimise tree selection, mostly based on modifications of this tree-selection algorithm, are given by Pukkala and Miina (1998). Assume that the tree dbh distribution can be divided into the three diameter classes small, medium and large. To simplify this classification, suppose that each class contains the same number of trees. Then once the current basal area exceeds a fixed basal stand value, the thinning operation is triggered. The number of trees to be removed from each class is specified a priori. Note that any type of thinning, either from above or from below, or any other tree selection criterium, can be simulated by defining the tree removal percentage from each class. Once the thinning method is defined, and the stand basal area that triggers the thinning is fixed, then the criterium of tree selection for each diameter class, and the order of tree removal have to be determined. This is based on the individual spatial competition pressure; trees most affected by spatial interaction are removed first, mimicking natural selection. Whilst if two competing trees are affected by equal spatial-interaction, then the smaller is removed.

To illustrate the effect of employing different thinning strategies, we first need to define suitable forest parameters in order to obtain qualitatively realistic forest dynamics. Suppose we consider a square forest stand of size 25×25 m^2 (i.e. 625/5,000 $\simeq$ 0.0625 ha) isolated from other stands, thereby ensuring edge effects. Let the initial population at time $t = 0$ comprise $n = 5{,}000$ trees/ha $\times$ 0.0625 ha $= 312$ trees distributed at random (i.e. seedlings follow a spatial Poisson distribution). This could be the result of either natural, or artificial, regeneration. Note that under regular rectangular spacing 312 trees corresponds to a $\sqrt{312} \times \sqrt{312} \simeq 17 \times 17$ array with nearest-neighbour distance of $25/17 \simeq 1.4$ m; so under random packing inter-tree distances should lie on either side of this value.

Let us further assume that: (i) initial mark radii are uniformly distributed over (0.25,0.75) cm for $i = 1,\ldots,n$; (ii) the maximum tree trunk rbh is $K = 25$ cm; and, (iii) the crown radius is $\delta = 9$ times larger than the trunk radius. Thus in terms of crown radius the initial $\delta m_i(0) \sim U(4.5,13.5)$ cm with $\max[\delta m_i(t)] = \delta K = 9 \times 25 = 225$ cm. Here, we presume that the radius of the zone of influence equals the crown radius, so the scale factor over the 25×25 m^2 stand is $r = 1$. Note, however, that if we simulate over the unit square then we have to take $r = 1/25$ in order to compensate for the reduced stand size. This choice of parameters provides representative values from a forest database involving several conifer tree species in the Catalan Pyrenees region in the North of Spain (presented by Gracia et al. 2003). Note that since under hard-core interaction (2.8), tree i's zone of influence has diameter $2\delta m_i(t)$, under rectangular maximum packing with each $\delta m_i(t) = \delta K = 9 \times 0.25$ m (assuming crown radius scaled to the 25×25 m^2 forest) there can be at most $[25/(2\delta K)]^2 = [25/(2 \times 9 \times 0.25)]^2 \simeq 31$ non-interacting trees over the 25×25 m^2 stand. So our 312 randomly distributed trees must be subject to considerable spatial competition.

To simplify this analysis, assume that: $\alpha \simeq 0$ (i.e. no "successful" immigration is expected); and, that the instantaneous death rate of a tree of size $m_i(t)$ is changed from the constant value μ to $\mu/\delta m_i(t)$, i.e. it is now dependent on tree size. For this ensures that small trees have a greater chance of dying naturally than large ones, which is clearly a more realistic assumption than assuming that natural mortality is independent of tree size. So on taking $\mu = 0.5$ the expected lifetime of a large isolated tree with crown radius $\delta m_i(t) = \delta K = 225$ cm is $\delta K/\mu = 450$ years, that for an established tree under competition with say $\delta m_i(t) = 100$ cm is 200 years, whilst that for a struggling small seedling of size 4 cm is a mere 8 years. All three values are realistic for the tree populations under study.

Note that in this process trees die both through (stochastic) "natural" mortality at rate $\mu/m_i(t)$ and (deterministic) interaction-induced mortality. So given this level of complexity there is little to be gained by defining a specific tree mortality submodel, where the number of trees to be eliminated and the specific trees to be removed are an explicit function of tree size, the number of trees in the stand, the stand basal area, and, a suitable competition index (as detailed, for example, in Kellomäki and Nevalainen 1983; Ojansuu et al. 1991). Here, the "self-thinning limit" (i.e. the highest possible number of trees contained in the forest stand) is a direct result of the deterministic growth and interaction components and the rate of random mortality.

We now have to select specific growth–interaction parameters. Suppose that individual trees develop in accord with the deterministic equation (2.1) formed by combining the VBCR growth function (2.5) and the area-interaction function (2.9). For in forest scenarios the latter provides a more realistic representation of reality than the hard-core function (2.8). Whence on taking $a_0 = \beta K^v/v$, $a_1 = 1-v$ and $a_2 = \beta/v$, Eq. (3.6) becomes

$$dm_i(t)/dt = (\beta m_i(t)/v)[(K/m_i(t))^v - 1] - b\theta. \qquad (5.1)$$

Moreover, in line with our earlier discussion on parameter values, let us take $K = 25$ cm together with the two

specific cases $v = 1$ and 0.7; recall that these correspond to linear and sigmoid growth, respectively. Now when $v = 1$ Eq. (5.1) reduces to

$$dm_i(t)/dt = (\beta K)(1 - m_i(t)/K) - b\theta, \tag{5.2}$$

which suggests placing $\lambda = \beta K$. Whence taking $\lambda = 1.3$ gives $\beta = 0.052$, and we shall retain this value for the $v = 0.7$ case. Also, let us choose the interaction parameter b to enable small trees to survive within the full shadow of at least one larger tree, since this ensures the existence of a genuine lower canopy structure. Now (3.6) implies that to have $dm_i(t)/dt > 0$ when $m_i(t) \simeq 1$ (say) and $\theta = 1$ requires

$$\begin{aligned} v = 1 \ : b &< \beta m_i[(K/m_i) - 1] = \beta K - \beta m_i \\ &= 1.3 - 0.052 m_i \simeq 1.25 \end{aligned} \tag{5.3}$$

$$\begin{aligned} v = 0.7 \ : b &< (\beta m_i/0.7)[(K/m_i)^{0.7} - 1] \\ &= (0.052/0.7)25^{0.7} m_i^{0.3} - (0.052 m_i/0.7) \simeq 0.63. \end{aligned} \tag{5.4}$$

So selecting $b = 0.6$ ensures that when $\theta \simeq 1$ small trees of size $m_i \simeq 1$ can survive under both values of v. Note, however, that whereas (5.2) shows that all small trees will survive when $v = 1$ (for $\theta = 1$), for $v = 0.7$ we do need $m_i > 0.789$ for survival in the lower canopy; hence tiny trees will soon die. Indeed, since the right-hand side of (5.1) takes the maximum value $(\beta K)(1 - v)^{-1+1/v} - b\theta$ at $m_i = K(1 - v)^{1/v}$, we need $b\theta < \beta K/(1 - v)^{-1+1/v}$ if *any* tree is to survive (i.e. have $dm_i(t)/dt > 0$) under this (b,θ)-regime. Finally, result (3.3) shows that after $t = 100$ years, isolated trees with small initial size, say $m_i(0) = 0.1$, reach size

$$\begin{aligned} m_i(100) &= K[1 + \{(1/250)^v - 1\}e^{-5.2}]^{1/v} \\ &= \begin{cases} 0.9945K & \text{at } v = 1 \\ 0.9923K & \text{at } v = 0.7. \end{cases} \end{aligned}$$

Thus for all practical purposes isolated trees have reached their maximum potential size after 100 years, which is the case for conifers. Our reason for comparing these two type of tree growth regimes is to study the effect that changing the growth function has on the resulting forest dynamics.

Finally, we select just two specific thinning strategies, from the huge number available, in order to illustrate how our modelling approach can provide considerable insight into the way in which choice of strategy can affect overall forest output. These two thinning programmes are: (1) a single-thinning regime from below with 100% and 50% of trees cut from small and medium diameter classes, respectively; and, (2) a two-thinning regime in which (1) is followed by a thinning from above which cuts 50% of trees from both the remaining medium and also the large diameter classes, respectively. Whilst the single thinning from below removes a large proportion of small and medium trees, thereby favouring the development of upper crown classes and increasing the economic value of forest products, the second thinning from above regulates tree competition by removing strong competitors, and hence favours an increase in individual tree size. The thinning from below is triggered when the basal area within our 25×25 m^2 stand reaches 3 m^2 (around year 7) in order to ensure an early control of tree density favouring the development of an upper crown class. Whilst the thinning from above is applied when the basal area reaches 6 m^2 (around year 15) in order to obtain an effective control on tree–tree competition. A final felling takes place at time $t = 100$. Note that in practice an optimal thinning strategy would be determined by conducting simulation experiments over all programmes deemed to be appropriate to the particular forest structure concerned.

Figure 1 shows the temporal development of population size over 100 years of forest growth, together with quadratic mean diameter $D(t)$, and stand basal area $G(t)$, for realisations based on the two growth functions, the two thinning regimes, and parameter values defined above. Such trajectories, together with the number of trees at time $t = 100$ (when the final felling is applied; see Table 1), highlight that under linear growth (i.e. $v = 1$) the population size is larger than that under sigmoid growth (i.e. $v = 0.7$) independently of the thinning programme. Note that this is in direct contrast to the temporal development of the quadratic mean diameter, since linear growth results in slightly smaller individual tree size, though larger basal area. Table 1 provides a measure of variability for such realisations by presenting (in brackets) the maximum and minimum associated values from 20 realisations of each scenario.

The behavioural differences between the two growth functions can be explained by noting that under $v = 1$ tree growth dominates spatial inhibition substantially more than under $v = 0.7$. For example, on paralleling the calculations leading to (3.7), we see that when $v = 1$ small trees of size $m \simeq 1$ can survive provided the canopy cover parameter $\theta < 2.08$, whilst when $v = 0.7$ the value is almost halved to $\theta < 1.05$. Thus under linear growth, interacting trees can initially reach larger sizes, and hence be less affected by random mortality at rate $\mu/m_i(t)$, than those under sigmoid growth. However, this initial reduction in tree mortality under linear growth produces a larger density of trees, which results in greater spatial competition. This in turn promotes smaller individual trees compared with those under sigmoid growth, where the higher initial tree mortality reduces tree population size, thereby resulting in larger values of $m_i(100)$. This is the reason why under linear, as compared to sigmoid, growth, there are a greater number of trees at the time of final felling, and although these are of slightly smaller individual size, the total basal area over the stand is greater.

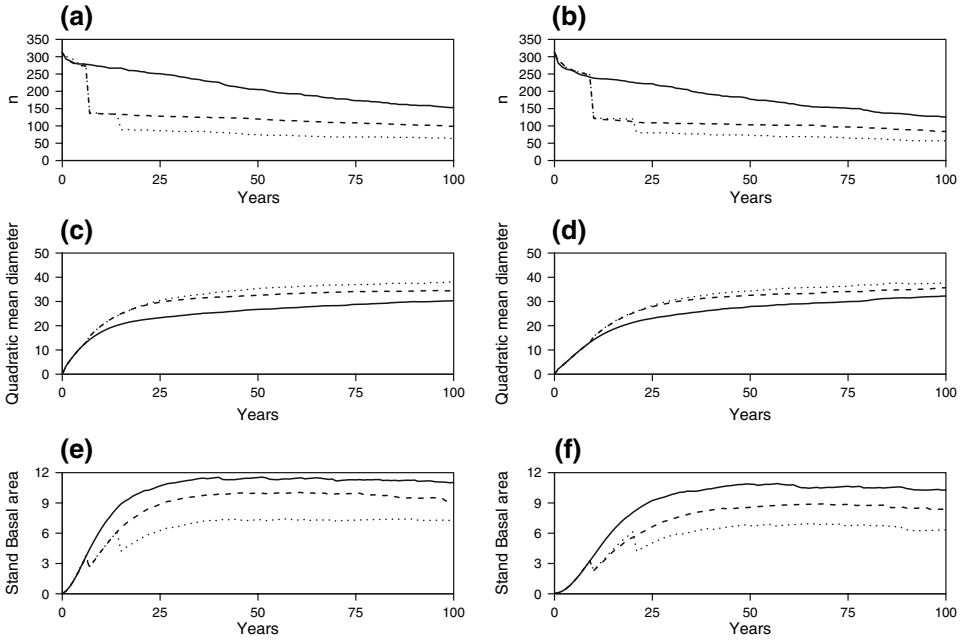

Fig. 1 Time–series plots for the growth–interaction model (2.1) based on the asymmetric area-interaction function (2.9) with $r = 0.01$ and $\delta = 9$, combined with the VBCR growth function (2.5) for $\beta = 0.052$, $K = 25$ and $b = 0.6$. The initial population comprises $n = 312$ trees with $U(0.25,0.75)$ radii at $t = 0$, $\mu = 0.05$ and $\alpha = 0$. Cases (**a**), (**c**) and (**e**) relate to $v = 1$, and (**b**), (**d**) and (**f**) to $v = 0.7$. Simulations are performed for a non-treated forest (*solid line*), a single-thinning from below (*dashed line*), and a two-thinning programme from below and above (*dotted line*). Quadratic mean diameter is given in cm and basal area in m^2 for a forest region of 0.0625 ha

Table 1 The year of thinning y, number of stems n, and stand basal area G (m^2 per 0.0625 ha) removed after thinning, the quadratic mean diameter D (cm), final felling (n, G and D) and the total biomass production (n and G) at $t = 100$ under: an untreated forest for $v = 1$ (A) and $v = 0.7$ (B); a single-thinning from below for $v = 1$ (C) and $v = 0.7$ (D); and a two-thinning programme for $v = 1$ (E) and $v = 0.7$ (F), corresponding to Fig. 1

	Thinning from below			Thinning from above			Final felling			Total	
	y	n	G	y	n	G	n	G	D	n	G
A	–	–	–	–	–	–	153	11.0	30.2	153	11.0
	–	–	–	–	–	–	(183–148)	(11.8–10.2)	(30.6–28.2)	(183–148)	(11.8–10.2)
B	–	–	–	–	–	–	126	10.2	32.2	126	10.2
	–	–	–	–	–	–	(143–121)	(10.8–10.1)	(32.6–30.4)	(143–121)	(10.8–10.1)
C	7	137	1.5	–	–	–	99	9.2	34.4	236	10.7
	(7–6)	(145–135)	(1.6–1.3)	–	-–	–	(111–88)	(9.8–8.2)	(36.0–33.4)	(256–223)	(11.4–9.5)
D	10	123	1.4	–	–	–	84	8.3	35.6	207	9.7
	(10–10)	(135–120)	(1.6–1.1)	–	–	–	(99–82)	(9.1–8.0)	(36.6–33.8)	(223–202)	(10.7–9.1)
E	7	140	1.6	15	45	2.2	64	7.3	38.0	249	11.1
	(7–7)	(143–132)	(1.7–1.5)	(16–15)	(46–42)	(2.3–2.1)	(77–58)	(8.3–6.6)	(38.2–35.6)	(266–232)	(12.3–10.2)
F	10	125	1.3	21	40	2.2	57	6.3	37.6	222	9.8
	(10–10)	(133–119)	(1.4–1.2)	(23–20)	(44–37)	(2.3–2.1)	(69–50)	(7.6–5.8)	(39.4–37.4)	(246–206)	(11.3–9.1)

Maximum and minimum values (in brackets) are shown from 20 realisations for each scenario

Nevertheless, despite producing different temporal development in population size, quadratic mean diameter and stand basal area, we see that the choice of tree growth function has only a small effect on the result of applying our two thinning strategies. When thinning from below, individual tree size is larger than that for a non-treated forest, suggesting that an early thinning contributes to a reduction in between-tree competition by allowing timber to be produced more efficiently. Indeed, the early control of tree density clearly has a considerable effect on individual tree size at the end of the rotation period (i.e. the total time a single forest is allowed to grow); compare the quadratic mean diameter values in Table 1.

A second thinning from above applied several years later contributes to increased individual tree size when compared to both the single-thinning from below scenario and the un-treated forest (see Fig. 1 and compare the quadratic mean diameter values in Table 1). For this second regulation of tree density further reduces between-tree competition, thereby further favouring the development of

larger individual trees. Note that the choice of growth model does not significantly affect the resulting dynamics for each thinning programme; the two-thinning regime always results in the better strategy if large individual trees are required. However, close inspection of Table 1 shows that the growth function does affect the thinning schedule. For under linear growth ($v = 1$) trees are thinned several years earlier than those under sigmoid curve ($v = 0.7$). This confirms that trees developing under linear growth initially experience less spatial inhibition, and hence grow faster, thereby reaching the stand basal area that triggers thinning before trees that develop under sigmoid growth.

Note that the variability of biomass production between the two models is far less than that between thinning schedules (see Fig. 1 and compare the total biomass production in terms of n and G in Table 1). This is particularly reassuring. For in practice we can only choose a process that, at best, provides a reasonable approximation to reality, and simulation results to date suggest that the approach is not unduly sensitive to model choice. Indeed, comparison of the resulting spatial configurations under linear and sigmoid growth at time $t = 100$ (see Figs. 2, 3), does not highlight any apparent (i.e. visual) structural difference between them, though under the former approach the number of trees contained in the stand is slightly larger than that contained in the latter. This is especially true in the untreated regime, where the resulting spatial patterns are substantially different from the thinned ones. From an academic viewpoint it would be interesting to conduct a formal space- and frequency-domain analysis of such simulated data (e.g. Cressie 1993; Renshaw 2002), though from a forestry perspective there is probably little practical value in such an undertaking given the broad similarities in forest outputs.

On a final point, in spite of the two-thinning approach maximising qmd and sba, Figs. 2c and 3c both exhibit empty space in which additional trees could exist without interacting with those already present. This highlights the danger in taking a purely formulaic approach to thinning, and demonstrates the need for a symbiotic relationship between method and forester when thinning strategies are being applied to forest stands.

6 Summary

Although thinning strategies play a fundamental role in the generation of spatial forest patterns, various forest studies have highlighted the difficulties involved in obtaining highly detailed experimental data in order to study their specific effects. Moreover, given that trees generally have an inherently long life-span relative to the length of typical research projects, experimenting with real forest stands is clearly of limited use. Fortunately, stochastic simulation through the development of a spatial–temporal process not only avoids such real-life complications, but the Renshaw and Särkkä (2001) technique of decomposing the process into a deterministic growth–interaction component and a stochastic birth–death component (later extended in Särkkä and Renshaw 2006), results in a computationally fast, and

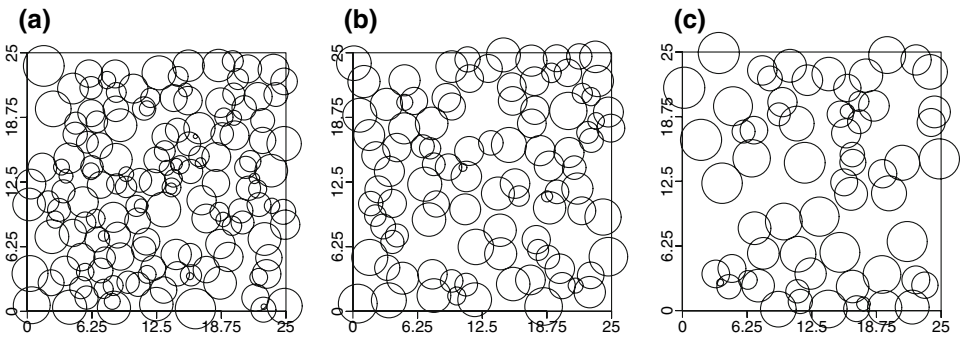

Fig. 2 Spatial structure shown at $t = 100$ corresponding to Fig. 1 under $v = 1$ for: **a** no thinning; **b** a single-thinning from below; and, **c** a two-thinning programme, first from below and then from above

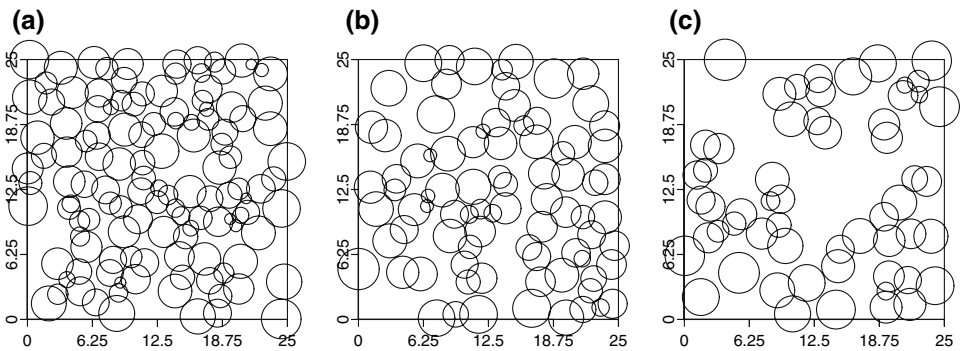

Fig. 3 As Fig. 2, but under $v = 0.7$

highly flexible algorithm, that can be easily adapted to cover any given scenario. This means that both new and established management strategies can be quickly analysed and compared.

Although here we have employed a simple immigration–death process over a homogeneous square region purely for the purposes of illustration, there is no reason why we could not replace: immigration by birth, or a specific planting regime; homogeneity by location-dependent parameters; and, the square boundaries by any general shaped region. Indeed, it is computationally trivial to extend the process to cover multi-species forests. Moreover, although we have also used the linear (2.2), logistic (2.2) and power-law (2.3) growth processes primarily for illustrative purposes, their close relationship to the highly applicable VBCR growth function (2.5) make them eminently useful in real-life situations. Indeed, when these are implemented in the general pair-wise growth–interaction model (2.1) they produce a powerful descriptor of forest growth that previous studies have shown to be particularly robust to exact model choice. This is a key feature, for it strongly suggests that provided the key elements of tree growth and interaction mechanisms are understood, the lack of further, more detailed, information should not significantly affect resulting inferences. The two interaction regimes considered, namely the symmetric hard-core interaction function (2.8) and its asymmetric soft-core area–interaction counterpart (2.9), cover a fairly wide range of possible situations, though any other interaction function, for example (2.10), could be used. Note that, if deemed appropriate, pair-wise interaction may be generalised to multi-point interactions without incurring too great a computational time penalty.

Earlier work in the stochastic simulation and analysis of biological pattern (Ford and Renshaw 1984; Henderson et al. 1983a, b) demonstrated the power of incorporating exact biological growth mechanisms into stochastic simulation routines. Bringing together the totally separate fields of forest management and spatial–temporal stochastic modelling on a much more formal basis would clearly represent a significant advance in the continuing development of applied science. Inputs from the former should play a major role in the construction of specific growth and interaction functions and the choice of model parameters, whilst both theoretical and computational developments in the latter are vital if we are to progress further the application of marked point processes in the real world. Here, for example, we have demonstrated how using three distinct thinning strategies (none, thinning from below, and thinning from below and then above) can have a substantial impact on forest outputs (e.g. number of trees, stand basal area and quadratic mean diameter). The next steps forward would first be to "fine-tune" the precise thinning mechanisms employed (timing, severity, etc.), followed by an investigation of all other likely contenders. Second, to recognise that as well as thinning, other management features of critical importance include planting regimes, construction of extraction routes, consideration of stand size, single- versus multi-species stands, etc. Our aim in this current paper has been to demonstrate the power and usefulness of this modelling approach, and to encourage its acceptance as a general forest modelling tool.

References

Banks RB (1994) Growth and diffusion phenomena. Springer, Berlin

Bella IE (1971) A new competition model for individual trees. For Sci 17:364–372

von Bertalanffy L (1949) Problems of organic growth. Nature 163:156–158

Chapman DG (1961) Statistical problems in dynamics of exploited fisheries populations. In: Proceedings of the 4th Berkeley symposium on mathematics, statistics and probability. University of California Press, Berkeley

Comas C (2005) Modelling forest dynamics through the development of spatial and temporal marked point processes. University of Strathclyde, Ph.D. thesis (unpublished)

Comas C, Mateu J (2006) Spatial clustering based on structured parent configurations: a perspective from reproducing individuals. Technical report 111, Universitat Jaume I, Castellon, Spain

Courbaud B, Goreaud F, Dreyfus Ph, Bonnet FR (2001) Evaluating thinning strategies using a tree distance dependent growth model: some examples based on the CAPSIS software "uneven-aged spruce forests" module. For Ecol Manage 145:15–28

Cressie NAC (1993) Statistics for spatial data (revised edition). Wiley, New York

Degenhardt A (1999) Description of tree distribution and their development through marked Gibbs processes. Biomet J 41:457–470

Diggle PG (2003) Statistical analysis of spatial point patterns. Arnold, London

Ek AR, Monserud RA (1974) FOREST: a computer model for simulating the growth and reproduction of mixed-species forest stands. Research paper, R2635. University of Wisconsin

Ferguson ER (1963) Overstory density key to pine seedling survival and growth in East Texas. J For 61:597–598

Ford ED, Renshaw E (1984) The interpretation of process from pattern using two-dimensional spectral analysis: modelling single species patterns in vegetation. Vegetation 56:113–123

Fritts HC (1976) Tree-ring and climate. Academic Press, New York

Gerrard DJ (1969) Competition quotient—a new measure of the competition affecting individual forest trees. Michigan State University Agricultural Experimental Station Research Bulletin, no. 20

Gracia CC, Burriel JA, Ibànez JJ, Mata T, Vayreda J (2003) Inventari Ecològic Forestal de Catalunya, 9. Bellaterra: CREAF

Hart HMJ (1928) Stamtal en Dunning–een Orienteerend Onderzoek naar de Beste Plantwijdte en Dunningswijze voor den Djati. Venman and Zonen, Wageningen

Hasenauer H (1994) Ein Einzelbaumwachstumssimulator für ungleichaltrige Fichten-Kiefern- und Buchen-Fichtenmischbestde. Forstliche Schriftenreihe der Universitä für Bodenkultur. Wien. Band 8, 152 pp

Hasenauer H, Moser M, Eckmüllner O (1995) MOSES: a computer simulation program for modelling stand response. In: Pinto da

Costa ME, Preuhsler T (eds) Mixed stands, research plots, and results, models. Instituto Superior De Agronomia, Universidade Tecnica de Lisboa, Portugal

Hawkes AG (1971a) Spectra and some self-exciting and mutually exciting point processes. Biometrika 58:83–211

Hawkes AG (1971b) Point spectra of some mutually exciting point processes. J R Stat Soc B 20:1–43

Hawkes AG (1972) Spectra of some mutually exciting point processes with associated variables. In: Lewis PAW (ed) Stochastic point processes. Wiley, New York, pp 261-271

Henderson R, Ford ED, Renshaw E, Deans JD (1983a) Morphology of the structural root system of Sitka Spruce. 1 Analysis and quantitative description. Forestry 56:121–135

Henderson R, Ford ED, Renshaw E (1983b) Morphology of the structural root system of Sitka Spruce. 2 Computer simulation of rooting patterns. Forestry 56:137–153

Kellomäki S, Nevalainen T (1983) On relationship between stand density and tree size. Silva Fennica 17:389–402

Lei YC, Zhang SY (2004) Features and partial derivatives of Bertalanffy–Richards growth model in forestry. Nonlinear Anal Modell Control 9:65–73

Mateu J, Usó JL, Montes F (1998) The spatial pattern of forest ecosystems. Ecol Modell 108:163–174

Matis JH, Kiffe TR, Matis TI, Stevenson DE (2007) Stochastic modeling of aphid population growth with nonlinear, power-law dynamics. Math Biosci 208:469–494

Matis JH, Kiffe TR, Parthasarthy PR (1998) On the cumulants of population size for the stochastic power law logistic model. Theor Popul Biol 53:16–29

Monserud RA, Sterba H (1996). A basal area increment model for individual trees growing in even-and uneven-aged forest stands in Austria. For Ecol Manage 80:57–80

Ojansuu R, Hynynen J, Koivunen J, Luoma P (1991) Luonnonprosessit metsälaskelmassa (MELA)- Metsä 2000-versio. Finnish Forest Research Institute Vantaa. Research paper 385

Oliver CD, Larson BC (1996) Forest stand dynamics. Wiley, New York

Pacala SW, Canham CD, Silander JA (1993) Forest models defined by field measurements: I. The design of a northeastern forest simulator. Can J For Res 23:1980–1988

Penttinen A, Stoyan D, Henttonen HM (1992) Marked point processes in forest statistics. For Sci 38:806–824

Pienaar LV, Turnbull KJ (1973) The Chapman–Richards generalization of von Bertalanffy's growth model for basal area growth and yield in even-aged stands. For Sci 34:804–808

Pretzsch H (1992) Konzeption und Konstruktion von Wuchsmodellem für Rein- und Mischbestände. Schriftenreihe d. Forstw. Fak. Univ. München, No. 115, 332 pp

Pretzsch H, Biber P, Ďursk J (2002) The single tree-based stand simulator Silva: construction, application and evaluation. For Ecol Manage 162:3–21

Prévosto B, Curt T, Gueugnot J, Coquillard P (2000) Modelling mid-elevation Scots pine growth on a volcanic substrate. For Ecol Manage 131:223–237

Pukkala T, Miina J (1998) Tree-selection for optimizing thinning using a distance-dependent growth model. Can J For Res 28:693–702

Pukkala T, Kolström T, Miina J (1994) A method for predicting tree dimensions in Scots pine and Norway spruce stands. For Ecol Manage 65:123–134

Pukkala T, Miina J, Kurttila M, Kolström T (1998) A spatial yield model for optimizing the thinning regime of mixed stands of *Pinus sylvestris* and *Picea abies*. Scand J For Res 13:31–42

Rathbun SL, Cressie N (1994) A space–time survival point process for a Longleaf pine forest in Southern Georgia. J Am Stat Assoc 89:1164–1174

Raulier F, Pothier D, Bernier PY (2003) Predicting the effect of thinning on growth of dense balsam fir stands using a process-based tree growth model. Can J For Res 33:509–520

Renshaw E (1984) Competition experiments for light in a plant monoculture: an analysis based on two-dimensional spectra. Biometrics 40:717–728

Renshaw E (2002) Two-dimensional spectral analysis for marked point processes. Biomet J 44:718–745

Renshaw E, Ford ED (1983) The interpretation of process from pattern using two-dimensional spectral analysis: methods and problems of interpretation. Appl Stat 32:51–63

Renshaw E, Särkkä A (2001) Gibbs point processes for studying the development of spatial–temporal stochastic processes. Comput Stat Data Anal 36:85–105

Richards FJ (1959) A flexible growth function for empirical use. J Exp Bot 10:290–300

Särkkä A, Renshaw E (2006) The analysis of marked point patterns evolving through space and time. Comput Stat Data Anal 51:1678–1718

Särkkä A, Tomppo E (1998) Modelling interactions between trees by means of field observations. For Ecol Manage 108:57–62

Smith DM, Larson BC, Kelty MJ, Ashton PMS (1997) The practice of silviculture; applied forest ecology. Wiley, New York

Staebler GR (1951) Growth and spacing in an even-aged stand of Douglas-fir. Master's thesis. University of Michigan

Stage AR (1973) Prognosis model for stand development. USDA Forest Service Research. Paper INT-137

Sterba H, Monserud RA (1997) Applicability of the forest stand growth simulator PROGNAUS for the Austrian part of the Bohemian massif. Ecol Modell 98:23–34

Stoyan D, Kendall WS, Mecke J (1995) Stochastic geometry and its applications. Wiley, New York

Teck R, Moeur M, Eav B (1996) Forecasting ecosystems with the forest vegetation simulator. J For 94:7–10

Tomppo E (1986) Models and methods for analysing spatial patterns of trees. Communicationes Instituti Forestalis Fenniae 138

Wahlenberg WG (1960) Loblolly pine. School of Forestry, Duke University

Wykoff WR, Crookston NL, Stage AR (1982) User's guide to the stand Prognosis model. USDA Forest Service General Technical Report INT-133

Zeide B (1993) Analysis of growth equations. For Sci 39:594–616